pubs.acs.org/Biomac Article

In Vitro and *In Vivo* Safety of Hyaluronic Acid-Decorated Microparticles for Intravitreal Injection of Palmitoylethanolamide, Citicoline, or Glial-Cell-Derived Neurotrophic Factor

Teresa Silvestri, Alejandra Daruich, Fatima Domenica Elisa De Palma, Valentina Mollo, Marie Christine Naud, Danilo Aleo, Fabiola Spitaleri, Guido Kroemer, Francine Behar-Cohen, Marco Biondi,* Emilie Picard,‡‡ Maria Chiara Maiuri,‡‡ and Laura Mayol‡‡

Cite This: *Biomacromolecules* 2023, 24, 3510−3521 Read Online

ACCESS | Metrics & More | Article Recommendations | Supporting Information

ABSTRACT: The treatment of posterior eye segment diseases through intravitreal injection requires repeated injections of an active molecule, which may be associated with serious side effects and poor patient compliance. One brilliant strategy to overcome these issues is the use of drug-loaded microparticles for sustained release, aiming at reducing the frequency of injections. Therefore, the aim of this work was to assess the safety features of poly(lactic-co-glycolic acid) (PLGA)-based, hyaluronic acid-decorated microparticles loaded with palmitoylethanolamide (PEA), citicoline (CIT), or glial-cell-derived neurotrophic factor (GDNF). Microparticles were prepared by double emulsion−solvent evaporation and fully characterized for their technological features. Microparticles possessed a satisfactory safety profile *in vitro* on human retinal pigment epithelial (ARPE-19) cells. Interestingly, the administration of free GDNF led to a loss of cell viability, while GDNF sustained release displayed a positive effect in that regard. *In vivo* results confirmed the safety profile of both empty and loaded microparticles. Overall, the outcomes suggest that the produced microparticles are promising for improving the local administration of neuroprotective molecules. Further studies will be devoted to assess the therapeutic ability of microparticles.

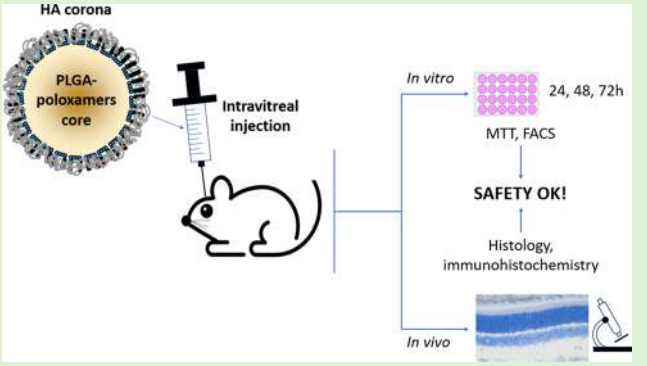

1. INTRODUCTION

There is an increasing necessity for improved therapeutic strategies in the treatment of posterior eye segment diseases such as diabetic retinopathy, age-related macular degeneration, uveitis, and glaucoma. In actual fact, these pathologies are chronic and progressive, and they are major causes of visual impairment worldwide[1,2] in elderly[3] and working-age patients.[4] To hinder the progression of these diseases, intravitreal (IVT) injection is still the preferred route of administration in clinical practice. Indeed, IVT injection allows direct access to the vitreous body and retina, thereby favoring therapeutically effective drug levels within the eye, along with a reduction of systemic side effects.[1,5] To provide a steady therapeutic regime, IVT injection is usually performed every 1−3 months according to the disease and the *in vivo* half-life of the chosen drug. Unfortunately, this often results in unsatisfactory patient compliance and high medical costs, as well as severe complications including retinal detachment, cataract, vitreous hemorrhage, and endophthalmitis, with an increasing chance of occurrence with an increasing number of injections.[6,7] Consequently, there is a clear-cut need for the design of sustained release systems to address the challenges associated with the existing therapy protocol for posterior eye segment diseases.

In this perspective, we have recently devised and produced biodegradable microparticles (MPs) for intraocular protein release, consisting of a core based on poly(lactic-co-glycolic acid) (PLGA) and externally decorated with hyaluronic acid (HA).[8−10] PLGA is a material of choice for the production of sustained release systems because it has been approved by the FDA for human use and is a generally regarded as safe (GRAS) material, also for ocular administration.[11] HA was selected as a coating for the outer surface of MPs due to its prominence in the vitreous body. This choice aimed at enhancing the connection between the MPs and the gel-like intraocular environment. Our previous findings substantiated this, showing that the presence of HA on the MP surface did hinder their

Received: March 17, 2023
Revised: June 29, 2023
Published: August 2, 2023

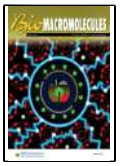

Downloaded via UNIV OF NAPLES FEDERICO II on December 16, 2024 at 15:14:28 (UTC).
See https://pubs.acs.org/sharingguidelines for options on how to legitimately share published articles.

ACS Publications © 2023 American Chemical Society

https://doi.org/10.1021/acs.biomac.3c00276
Biomacromolecules 2023, 24, 3510−3521

movement within the simulated vitreous body. This hindrance was attributed to the promoted interactions between the HA on the MPs and the HA in the gel.[12,13] This is important since it is expected to reduce the unrestricted MP diffusion within the vitreous, which may interfere with visus.[8] In this work, MPs were loaded with three active molecules, namely palmitoylethanolamide (PEA), citicoline (CIT), and glial-cell-derived neurotrophic factor (GDNF), which were chosen for their expected neuroprotective effect on injured inner retina.[14−16] PEA is a poorly water-soluble endogenous analogue of the endocannabinoid anandamide, endowed with a potent anti-inflammatory activity, that has been shown to attenuate the degree of retinal inflammation[17] and optimize visual field of glaucoma patients while decreasing intraocular pressure (IOP).[18] CIT acts as an intermediate in the synthesis of membrane phospholipids and is involved in the preservation of cellular homeostasis.[15] In addition, its neuroprotective effect in neurological diseases such as stroke[19] and brain injuries[20] is known. CIT may play a role in the treatment of ophthalmological diseases such as amblyopia, optic neuropathies, glaucoma, and diabetic retinopathy.[21,22] Indeed, the ability of CIT to neutralize the excitotoxicity due to the action of glutamate on damaged retinal ganglion cells (RGC) has been shown both *in vitro* and *in vivo*.[23,24] GDNF is a protein belonging to a family of ligands, which play a crucial role in the development and function of the nervous system and renal growth.[25] It has been demonstrated that GDNF has a neuroprotective effect on photoreceptors and RGCs.[26] Previous studies were mainly focused on the evaluation of GDNF loaded in MPs, along with the technological characterization of the *in vitro* and *in vivo* model devices.[27,28]

The aim of this study was to assess the ocular safety profile of the produced MPs *in vitro* and *in vivo*. The devices were characterized for their technological features and their effects on human retinal pigment epithelial (ARPE-19) cells evaluated by the 3(4,5-dimethylthiazol-2-yl)-2,5-diphenyltetrazolium bromide (MTT) conversion assay and cytofluorometric assessment of apoptosis to verify the cell viability. Finally, the *in vivo* response was assessed by histological and immunohistochemical analysis in the rat retina.

2. MATERIALS AND METHODS

2.1. Materials. Poly(D,L-lactide-co-glycolide) (PLGA) (Supporting Figure 1C) (Resomer RG504H lactide/glycolide ratio of 50:50; inherent viscosity: 0.57 dL/g in chloroform at 25 °C) was purchased from Evonik (Essen, Germany). Hyaluronic acid (HA; Supporting Figure 1D; M_w: 1.6 MDa; viscosity > 1.5 mm^2/s) was provided by DSM (Kaiseraugst, Switzerland). Two poloxamers (PEOa-PPOb-PEOa) were employed: F127 (a = 100 and b = 65) and F68 (a = 76 and b = 29). They were provided by Sigma Aldrich like the following other chemicals: bovine serum albumin (BSA), dichloromethane (DCM), sodium phosphate (Na_2HPO_4), potassium chloride (KCl), sodium chloride (NaCl), human GDNF (glial-derived cell neurotrophic factor), ELISA kit, dimethyl sulfoxide (DMSO), palmitoylethanolamide (PEA) (Supporting Figure 1B), 3-(4,5-dimethylthiazol-2-yl)-2,5-diphenyltetrazolium bromide (MTT), and modified Eagle's/F-12 medium (DMEM/F-12). Citicoline (CIT) (Figure S1A) was purchased from ACEF (Italy). Fetal bovine serum (FBS), penicillin, streptomycin, and trypsin−EDTA were obtained from Gibco. Acetonitrile (ACN) HiPerSolv-CHROMANORM and HPLC-grade water were obtained from VWR. Disodium phosphate dodecahydrate $Na_2HPO_4{\cdot}12H_2O$ and sodium phosphate dihydrate $NaH_2PO_4{\cdot}2H_2O$ were purchased from Farmalabor (Italy). 3,3′-Dihexiloxalocarbocyanine iodide (DiOC6(3)) was obtained from Molecular Probes, Life Technologies. 4′,6-Diamidino-2-phenylindole (DAPI) and donkey anti-mouse antibodies were provided by ThermoFisher. Ketamine 1000 was purchased from Virbac, (Carros, France), while Rompun 2% from Bayer Santé (Puteaux, France), mydriaticum 0.5% from Thea (France), and tetracaine 1% from Faure (France). Paraformaldehyde and glutaraldehyde were obtained from LADD, Inland Europe (Conflans-sur-Lanterne, France). Finally, the Leica Historesin Embedding Kit was provided by Leica (Switzerland) and rabbit anti-glial fibrillary acidic protein (GFAP) was obtained from Dako (Trappes, France). All of the chemical substances were used without any purification.

2.2. MP Formulation Method. MPs were fabricated by a slightly modified double emulsion−solvent evaporation technique, with no chemical reaction, following a previously published procedure.[8−10] Briefly, unloaded MPs (named MP EMPTY) were produced by emulsifying 0.25 mL of an internal aqueous phase (W_0) (consisting of a BSA solution 0.4% w/v in phosphate buffer) with 2.5 mL of PLGA/F68/F127 (1:0.5:0.5 weight ratio) solution in methylene chloride (overall polymer concentration: 20% w/v) using a high-speed homogenizer (Diax 900 equipped with a 10G probe, Heidolph, Germany; 11 000 rpm, 2 min). The obtained W_0−O primary emulsion was poured in 40 mL of an external aqueous phase (W_1) containing two poloxamers (F68 and F127; 0.0375 mg/mL respectively) and HA (0.75 mg/mL; M_w:1600 kDa), and further homogenized at 11 000 rpm (10G probe) for 2 min, to obtain the final W_0−O−W_1 multiple emulsion. The organic solvent was evaporated overnight under magnetic stirring (500 rpm, RT), and the hardened MPs were centrifuged at 4 °C (5000 rpm, Universal 16R, Hettich Zentrifugen, Germany), washed with double distilled water three times and lyophilized for 24 h (−80 °C, 0.1 mbar, 24 h; LyoQuest, Telstar, Japan). The W_0 phase contained 125 mg of CIT or 10 μg of GDNF, while 6.3 mg of PEA were solubilized in the O phase.

2.3. Microparticle (MP) Characterization. MP size and size distribution were determined by laser diffraction (Mastersizer 3000E, Malvern Panalytical, Malvern, UK). MPs were dispersed in double distilled water under continuous stirring at 1500 rpm (λ = 632.8 nm). The mean diameters and the standard deviation were expressed as averaged triplicate samples. To provide a measure of the size distribution of the produced MPs, SPAN values were calculated by formula (1)

$$\text{SPAN} = \frac{d(90\%) - d(10\%)}{d(50\%)} \tag{1}$$

where $d(n\%)$ is the diameter at the percentile n of the cumulative distribution.[29]

Scanning electron microscopy (SEM) (Ultraplus Zeiss) was employed to analyze MP external shape and morphology. To this aim, lyophilized MPs were mounted on a metal stub with double-sided tape and coated with gold for 30 s under an argon atmosphere using a plasma sputter. SEM acquisitions were performed at an accelerated voltage of 15 kV and a magnification of 2000 times.

MP yield was gravimetrically obtained from the entire mass of MPs recovered after lyophilization using formula (2)

$$\text{yield\%} = \frac{\text{weight of freeze dried MPs}}{\text{total amount of PLGA + active molecules}} \times 100 \tag{2}$$

Entrapment efficiency was determined by the direct method. In the case of PEA or CIT-loaded MPs, 1.7 or 1.25 mL of the MP suspension were placed in a volumetric flask after centrifugation, and acetonitrile was added to a final volume of 10 mL for dissolution of MPs. Then, CIT or PEA was quantified using a high-performance liquid chromatography (HPLC) (Agilent series 1200) system equipped with a G1314B UV detector.

The mobile phase was prepared by pouring 2.5 g of disodium phosphate dodecahydrate into 700 mL of HPLC-grade water and stirring until dissolution. Then, sodium phosphate dihydrate (0.5 g) was added and, if necessary, the pH of the solution was adjusted to pH = 7.4. Finally, water was added to a final volume of 1 L. The

https://doi.org/10.1021/acs.biomac.3c00276
Biomacromolecules 2023, 24, 3510−3521

obtained solution was filtered through 0.2 μm cellulose acetate filters. The running conditions for HPLC tests are reported in Table 1.

Table 1. Equipment and Experimental Conditions of PEA and CIT MP Entrapment Efficiency

	MP PEA	MP CIT
mobile phase	(**A**) ACN; (**B**) phosphate buffer pH:7.4	(**A**) ACN; (**B**) sodium phosphate dihydrate solution 10 mM
elution mode	Isocratic: 65% (**A**) − 35% (**B**)	Isocratic: 10% (**A**) − 90% (**B**)
flow rate	0.6 mL/min	1 mL/min
injection volume	4 μL	10 μL
λ	210 nm	274 nm
column temperature	25 °C	25 °C
run time	10 min	15 min
Rt	3.9 min	9.8 min

To find out the entrapment efficiency of GDNF, lyophilized MPs (5 mg) were dissolved in 0.7 mL of DCM and 0.7 mL of a 1% w/v BSA in PBS solution (pH = 7.4) was added. Then, the samples were vigorously vortexed for 1 min and centrifuged for 15 min (11 300 rpm, 24 °C; MKRO 200R, Hettich). Afterward, the supernatant was removed and further 0.7 mL of 1% w/v BSA in PBS solution was added to the organic phase. The sample was centrifuged three more times under the same conditions and GDNF was quantified by an ELISA test, employing a Human GDNF ELISA Kit. The linearity of the response was assessed in the 2.24−222 pg/mL GDNF concentration range (R^2 > 0.995). The entrapment efficiency and loading capacity were calculated employing eqs (3) and (4)

$$\text{entrapment efficiency\%} = \frac{\text{amount of encapsulated drug}}{\text{total amount of drug}} \times 100 \quad (3)$$

$$\text{loading capacity\%} = \frac{\text{amount of encapsulated drug}}{\text{total amount of polymer}} \times 100 \quad (4)$$

In vitro release kinetics of GDNF, PEA, and CIT were assessed as described in our previous work.[8−10] Briefly, lyophilized MPs loaded with GDNF, CIT, or PEA were suspended in a simulated vitreous body (SVB) (1:20 weight ratio) and 1 mL of PBS was added. The samples were placed in a thermostatic bath at 37 °C and at pre-established time points (once a week until 57 days) aliquots of the supernatant PBS were recovered, replaced with the same volume, and analyzed by ELISA to determine GDNF released content and by HPLC to evaluate the amount of PEA and CIT released from MP GDNF, MP PEA, and MP CIT, respectively. For all tests, results were expressed as the mean values ± the standard deviation of triplicate experiments.

2.4. Cell Culture. Human retinal Pigment epithelial ARPE-19 (ATCC-CRL-2302) cells were cultured in the DMEM/F-12 medium supplemented with 10% v/v FBS, 100 U/mL penicillin, and 100 μg/mL streptomycin. The cells were seeded in 75 cm^2 flasks and placed in a humidified atmosphere at 37 °C with 5% CO_2 and then passaged once a week using 0.25% Trypsin−EDTA. The FBS concentration was lowered to 1% to perform experiments.

2.5. MTT Assay. The cell viability was determined using the 3-(4,5-dimethylthiazol-2-yl)-2,5-diphenyl-2*H*-tetrazolium bromide (MTT) conversion assay. ARPE-19 cells were cultured in 96-well plates and plated at 2 × 10^4 cells per well. Then, they were grown to 80% confluence before carrying out the experiments. After the stimulation with empty MP, drug-loaded MPs, and active molecules alone employing different concentrations (Table 2) for 24, 48, and 72 h, the cells were incubated with 20 μL of MTT solution (5 mg/mL) for 4 h at 37 °C. Then, the formed formazan crystals were dissolved in 200 μL of DMSO and incubated for 15 min. The absorbance of each well was measured at 570 and 750 nm, which served as the reference wavelength, using a microplate reader (Victor, PerkinElmer). Cell viability was expressed as the percentage of living cells with respect to the untreated control. The % cell viability has been calculated as follows

Table 2. Employed Concentration of Empty MPs, Drug-Loaded MPs, and Active Molecules Alone as Stimulation Treatment of the ARPE-19 Cells

concentration of empty and drug-loaded MPs (mg/mL)	concentration of PEA alone (mg/mL)	concentration of CIT alone (mg/mL)	concentration of GDNF alone (mg/mL)
C3: 5 × 10^{-4}	C3: 2 × 10^{-4}	C3: 2 × 10^{-4}	C1: 5 × 10^{-4}
C4: 5 × 10^{-6}	C5: 2 × 10^{-8}	C5: 2 × 10^{-8}	C2: 5 × 10^{-6}
C5: 5 × 10^{-8}			C3: 5 × 10^{-8}

$$\%\text{viability} = \frac{\text{mean OD sample}}{\text{mean OD blank}} \times 100 \quad (5)$$

The IC_{50} values for each compound were determined by first assessing cell viability through the extraction of OD values from the MTT assays. Subsequently, linear regression curves were utilized to calculate the IC_{50} values, as shown in eqs 6 and 7.

$$y = (ax + b) \quad (6)$$

$$IC_{50} = \frac{50 - b}{a} \quad (7)$$

2.6. Cytofluorometric Assessment of Apoptosis. ARPE-19 cells were cultured in the same conditions described in Section 2.4. The cells were stimulated with empty MPs, drug-loaded MPs, active molecules alone (Table 2), and cisplatin (500 μM) for 24 h. Thereafter, for apoptosis determination, cells were harvested and stained for 30 min at 37 °C with the following: (i) 20 nM $DiOC_6(3)$ for mitochondrial transmembrane potential (ΔΨm) quantification and (ii) 1 μg/mL DAPI, a dye that incorporates only into dead cells and is used for the determination of cell viability. Cytofluorometric acquisitions were performed on a Miltenyi flow cytometer (MACSQuant Analyzer 10) gating 6000 events per sample. Data (FITC/VioBlue data) were analyzed using FlowJo software.

2.7. Animal Procedures. Thirty-nine male Wistar albino rats (Janvier, Le Genest Saint-Isle, France; age: 8 weeks) were used in accordance with the EU Directive 2010/63/EU for animal experiments and followed the ARVO Statement on the Use of Animals in Ophthalmic and Vision Research. Furthermore, studies were approved by the local ethics committee "Charles Darwin" (#20648, 2019). Animals were fed with a standard laboratory diet and ad libitum tap water at a controlled room temperature of 21−23 °C. The cyclic light environment consisted of 12 h of light per day. Three rats were used as control without injection, and all eyes were used for histological examination. At the time of the experiment, rats were 10 weeks old and were anesthetized by intramuscular injection of 100 μL/100 g ketamine solution (40 mg/mL) and xylazine (4 mg/mL). Topical ocular anesthesia with one drop of tetracaine hydrochloride (Tetracaine 1%, Faure, Europhta Laboratories, Monaco) was performed 2 min before the injection. Pupillary dilatation was obtained by instillation of two drops of 2 mg/0.4 mL mydriaticum (Théa, Clermont-Ferrand, France) and 10% phenylephrine hydrochloride (Faure, Europhta Laboratories, Monaco). 5 μL of MP suspension was administered superiorly into the vitreous body using a 31G needle for insulin (100 U). Injections were performed under an operating microscope by an ophthalmic surgeon and by placing a microscope slide on the cornea to allow fundus observation.[30]

Animals that received intravitreal injections in both eyes of drug-loaded MPs were randomized into four groups (n = 16): CIT, PEA, and GDNF with dosages of 3.1, 0.32, and 47.6 ng, respectively, and empty MPs as the control.

For the MP injection procedure, 66% (w/v) suspensions of MPs were prepared in balanced salt solution (BSS) and briefly vortexed

https://doi.org/10.1021/acs.biomac.3c00276
Biomacromolecules 2023, 24, 3510−3521

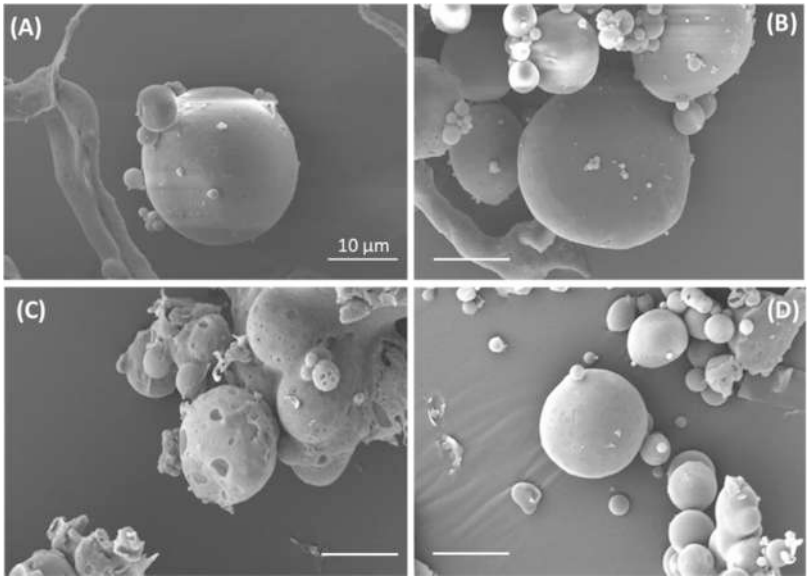

Figure 1. Representative SEM images of MPs: (A) EMPTY, loaded with GDNF (B), CIT (C), or PEA (D).

Table 3. Summary of Technological Features of Unloaded (Empty) and Loaded MPs with PEA, CIT, and GDNF[a]

formulation	mean diameter (μm) ± SD	SPAN ± SD	E.E. (%) ± SD	L.C. (%) ± SD
MP EMPTY	27 ± 2.0	3.1 ± 2.1		
MP CIT	28 ± 2.0	2.9 ± 1.9	19 ± 8.0	8.0 ± 5.1
MP PEA	26 ± 3.0	3.3 ± 1.3	9.0 ± 6.0	2.1 ± 0.7
MP GDNF	39 ± 6.0	2.2 ± 1.8	68 ± 5.0	0.1 ± 2.3

[a]The results are expressed as the mean value ± SD calculated on at least three repeats.

immediately before each injection to ensure homogeneity of MPs in the injected suspension. 5 μL of MP suspension were administered superiorly into the vitreous body using a 31G needle for insulin (100 U). After seven days, animals were euthanized by carbon dioxide inhalation and both eyes were immediately enucleated with a piece of tissue at the superior area for right orientation, one treated for histology and the other one for immunohistochemical staining.

2.8. Histology. One eye from each rat was fixed with 4% v/v paraformaldehyde and 0.5% v/v glutaraldehyde in PBS for 2 h for histological analysis. After fixation, samples were washed and dehydrated in a graded alcohol series: 2 h in 70% alcohol and 2 h in 95% alcohol. Then, a mixture of the infiltration medium and 95% alcohol for 2 h was employed. Finally, the samples were incubated in the infiltration solution of the Leica Historesin Embedding Kit overnight at 4 °C. Samples were embedded in the embedding medium and attached to a block holder after polymerization. A plastic section (5 μm thick) passing through the optic nerve head were prepared on a microtome (Leica Microsystems, France), stuck on slides, and stained for 15 min with 1% w/v toluidine blue solution. Sections were observed with a microscope (Leica Microsystems, Switzerland) and photographed with a Leica Microsystems camera.

2.9. Retina Thickness Measurement. The thicknesses of the outer nuclear layer (ONL), inner nuclear layer (INL), and photoreceptors segments were measured every 500 μm on the section passing through the center of the optic nerve using ImageJ software (1.53 k; bundled with Java 64-bit, 1.8.0.172). Measurements of histological sections were performed across the whole retina, considering the inferior pole to 0 from −4000 μm from the optic nerve and the superior pole from 0 to 4000 μm from the optic nerve. Thickness profiles along the retina were generated by averaging, for each distance, the values obtained for all eyes treated similarly to give a single value per group.

2.10. Immunohistochemical Analysis. The other eye for each rat was fixed with 4% v/v paraformaldehyde in PBS for 2 h, washed with PBS, and infiltrated in gradient sucrose series diluted in PBS (10% w/v, then 20% w/v and finally 30% w/v for 2 h each). Then, the eyes were further mounted on Tissue-Tek O.C.T. (Siemens Medical, Puteaux, France) and frozen with dry ice. Frozen sagittal sections (10 μm) close to the optic nerve were cut using a microtome (Leica). The sections were washed and permeabilized with 1% v/v Triton X-100 for 30 min. After rinsing with PBS, the cryo-sections were incubated for 1 h at room temperature with different primary antibodies (GFAP, 1:200 and CD11b, 1:100) diluted in a primary antibody solution of 0.1% v/v Triton X-100 in PBS. Negative control sections were incubated without primary antibodies. After washing with PBS, the sections were incubated for 1 h with secondary antibodies coupled with a fluorochrome (goat anti-rabbit 1:200) and donkey anti-mouse, 1:200 in a secondary antibody solution (0.1% v/v Triton X-100 in PBS). Finally, after the rinsing with PBS, slides were stained for the nuclei with DAPI (1:5000) for 5 min, washed again, and mounted with a gel mount. Fluorescently labeled sections were observed under an epifluorescence microscope (Olympus, Rungis, France) equipped with a CCD camera (Olympus DP72) using identical exposure parameters across samples to be compared. To evaluate activated macrophages/microglial cells, GFAP, and CD11b level intensity were measured on pictures acquired over the entire ocular cross sections at the optic nerve level. Both GFAP and CD11b level intensities were measured using ImageJ software. Intensity values were generated by averaging the values obtained for all pictures treated similarly to give a single value per group.

2.11. Statistical Analyses. Statistical analyses were performed using GraphPad Prism 8.0.3 software. Statistical significance was defined at $*p < 0.05$, $**p < 0.01$, and $***p < 0.001$ by using one-way or two-way ANOVA completed with Dunn's, Dunnet's, Kruskal–Wallis, Tukey's or Sidak's testing for multiple comparisons. All results are presented as mean ± standard deviations (SD) or standard error of the mean (SEM, as mentioned in the figure legends).

https://doi.org/10.1021/acs.biomac.3c00276
Biomacromolecules 2023, 24, 3510−3521

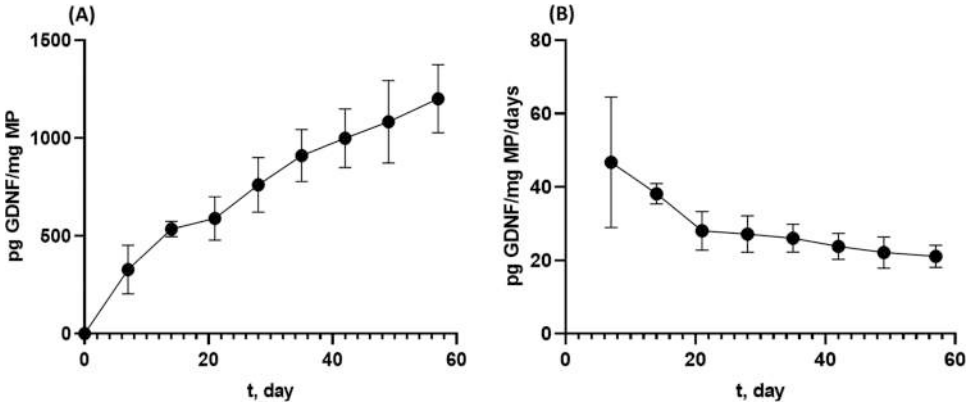

Figure 2. Cumulative release of GDNF from HA-decorated MPs in the simulated vitreous body at 37 °C. They are expressed as pg of GDNF released from 1 mg of microparticles (A) or as the rate of GDNF release (pg/mg MP/day) (B). Results are expressed as the mean ± SD of three replicates.

3. RESULTS

3.1. Technological Characterization of Microparticles.

3.1.1. Morphological Analyses. MP morphology was studied by SEM (Figure 1). In all formulations, spherical particles were obtained. In the case of empty, GDNF- and PEA-loaded MPs, a smooth surface was observed. Interestingly, SEM images showed that the surface of CIT-loaded MPs exhibited noticeable pores.

3.1.2. Dimensional Analysis, Entrapment Efficiency (E.E.), and Loading Efficiency (L.C.) of MPs. The produced MPs were loaded with three active molecules, palmitoylethanolamide (PEA), citicoline (CIT), and glial-cell-derived neurotrophic factor (GDNF). The mean diameter, entrapment efficiency (E.E.), SPAN, and loading capacity (L.C.) of all of the obtained MPs are summarized in Table 3.

The mean diameter of MPs was between 27 and 39 μm. Even if the employed technique for MP production was the same for all formulations, the entrapment efficiency was dependent on the loaded molecule, ranging from 9 to 68%. Correspondingly, the drug:polymer weight ratio was 0.0475, 0.00114, and 0.00002 for CIT, PEA, and GDNF, respectively.

3.1.3. In Vitro Drug Release. We analyzed the cumulative *in vitro* release profile of GDNF from MPs in SVB, expressed as pg of active molecule per mg of MPs as a function of time (Figure 2A). After 7 days, the delivered GDNF was 327.1 ± 13.2 pg GDNF/mg MPs. Subsequently, a near-zero order GDNF release was observed up to 57 days, with an approximately constant rate of 26.62 ± 5.70 pg GDNF/mg MP/day until the last time point of observation (57 days) (Figure 2B).

The investigation of *in vitro* release kinetics of PEA and CIT from MPs revealed that both the active molecules were released in a span of approximately two weeks (data not shown). In this regard, our data underscored that the release of these drugs lacked adequate control. Consequently GDNF, among other candidates, emerged as a preferable active molecule for loading in the MPs.

3.2. Effects of Empty and Loaded MPs on Cell Viability.

To assess the toxicity of the MPs *in vitro*, we used the human retinal pigment epithelial (ARPE-19) cells to perform MTT and cytofluorometric analysis.

For the MTT assay, ARPE-19 cells were treated with different concentrations of empty MPs, bare active molecules, and active molecule-loaded MPs. In all experimental conditions, the viability of untreated cells was comparable to that of the other groups, therefore confirming that the empty or loaded MPs are not toxic (Figure 3). Contrariwise, at each time point considered, cisplatin,[31] used as the internal positive control of the experiment, induced significant cell death. Interestingly, the cells treated with MPs loaded with GDNF presented a significantly higher viability with respect to the cells incubated with GDNF alone. This is ascribable to the slow release of GDNF from MPs (Figure 3).

Next, in order to corroborate the non-toxicity of MP treatments on ARPE-19 cells, we carried out a cell death assay using flow cytometry. ARPE-19 cells were treated for 24 and 72 h with several concentrations of empty and drug-loaded MPs and cisplatin, used as an internal positive control of the experiment using untreated cells as control (Ctrl group). After 24 and 72 h of treatment, cells were stained with the $\Delta\Psi_m$-sensitive dye $DiOC_6(3)$ and DAPI (Figure 4A,B). All of the treatments did not induce cell death, confirming the MTT test outcomes, except for cells treated with cisplatin, at both time points (Figure 4). These results were also confirmed by the estimation of the IC_{50} values of empty and loaded MPs in ARPE-19 cells determined after 24, 48, and 72 h of treatment (Table 4).

3.3. Safety Assessment of MP Formulations *In Vivo*.

Based on the results concerning the absence of toxicity of all MP formulations *in vitro*, we decided to test them *in vivo* to evaluate their potential toxicity in the rat posterior segment eye tissues. Animals, randomized into four groups (n = 16), received intravitreal injection (IVT) of empty MPs and three different MP formulations loaded with the active molecules (CIT: 3.1 μg; PEA: 0.32 μg, and GDNF: 47.6 ng), in both eyes.

We evaluated the effects of all MPs on retina thickness measurement. The evaluation of the outer nuclear layer (ONL), inner nuclear layer (INL), and photoreceptor segment thickness showed that all MPs did not affect the architecture of the retina (Figure 5). The ONL and INL thicknesses were not significantly different from control rats and when compared with those injected with both loaded and unloaded MPs.

To corroborate these results, we also evaluated, in the same treatment groups, the expression of GFAP (anti-glial fibrillary acidic protein) and CD11b by immunohistochemistry. GFAP is usually expressed by astrocytes in the normal retina, while it is also expressed in activated Müller glial cells when gliosis is present in the retina, reflecting retinal stress.[32] CD11b is a

https://doi.org/10.1021/acs.biomac.3c00276
Biomacromolecules 2023, 24, 3510−3521

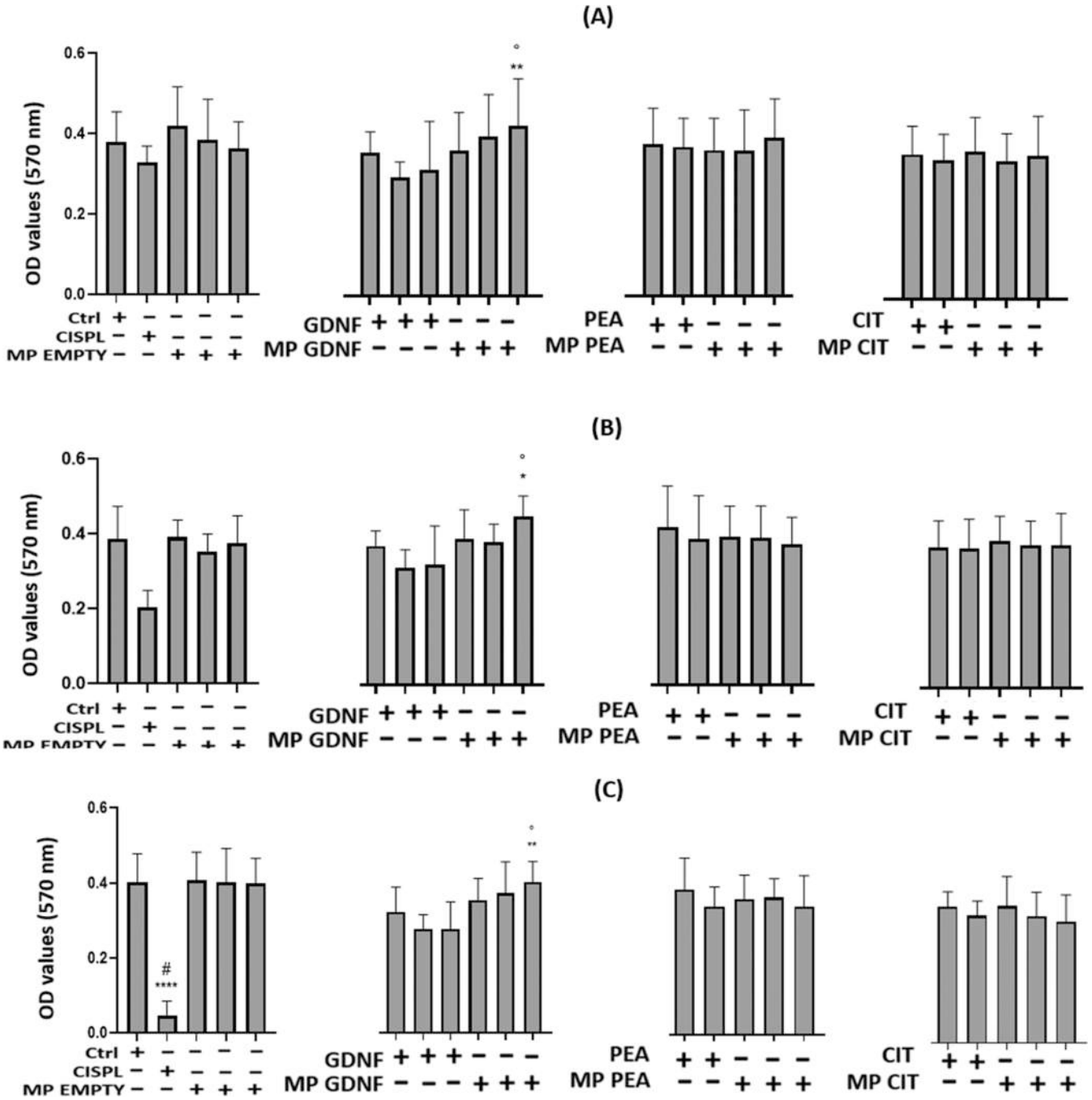

Figure 3. Effect of different MP formulations on ARPE-19 cell viability. Cells were treated with different concentrations of MPs unloaded (EMPTY) or loaded with molecules. MTT assay was performed at 24 (A), 48 (B), and 72 (C) h after the treatment. Results are from four independent experiments with four parallel samples per group in each experiment and shown as mean ± SEM. Ctrl = control; CISPL = cisplatin, 500 μM; CIT = citicoline; PEA = palmitoylethanolamide; and GDNF = glial-cell-derived neurotrophic factor. Statistical analysis was performed by Kruskal−Wallis's test with Dunn's test for multiple comparisons, $n = 3$; *$p < 0.05$, **$p < 0.01$, ****$p < 0.0001$ when compared to control conditions; °$p < 0.05$ when compared MPs GDNF to equivalent concentrations of GDNF alone. The concentration of EMPTY MPs and loaded MPs is: C3 = 5×10^{-4} mg/mL, C4 = 5×10^{-6} mg/mL, and C5 = 5×10^{-8} mg/mL. The concentration of active molecules alone is: PEA C3 = 2×10^{-4} mg/mL, PEA C5 = 2×10^{-8} mg/mL, CIT C3 = 2×10^{-4} mg/mL, CIT C5 = 2×10^{-8} mg/mL; GDNF C3 = 5×10^{-4} mg/mL, GDNF C4 = 5×10^{-6} mg/mL, and GDNF C5 = 5×10^{-8} mg/mL.

marker for macrophages; in the retina, CD11b stained resident retinal macrophages, the microglia, and infiltrated macrophages.[33] In the absence of stress or degeneration, microglial cells exhibit a ramified morphology with a small, round soma, and various branching processes. Once activated, they proliferated and gained shorter processes and an ameboid form. In our experimental setting, we did not observe any significant gliosis or inflammation throughout the retina, due to the lack of activation of Müller glial cells and microglia cells. In all treatment groups, the GFAP signal was only limited to astrocytes in ganglion cell layer (GCL) and CD11b microglia cells were only localized in the inner retina with a steady-state phenotype (Figure 6). CD11b and GFAP signal intensity were

https://doi.org/10.1021/acs.biomac.3c00276
Biomacromolecules 2023, 24, 3510−3521

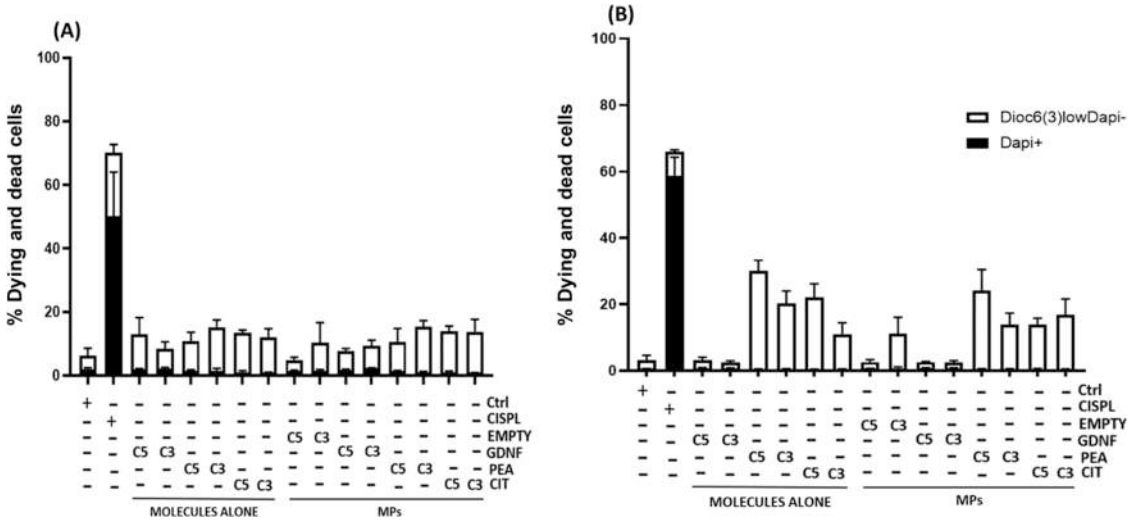

Figure 4. Effect of different MP formulations on cell death at 24 (A) and 72 h (B). ARPE-19 cells were treated as indicated and then double-stained with $DiOC_6(3)$ and DAPI. The black portions of the columns refer to $DAPI^+$ population (dead) and the remaining part of the column corresponds to the $DiOC6(3)^{low}/DAPI^-$ (dying) population. Columns indicate means ± SD. Figures are representative of one experiment where each condition has been performed in triplicate. Ctrl = control; CISPL = cisplatin, 500 μM. CIT = citicoline, PEA = palmitoylethanolamide, and GDNF = glial-cell-derived neurotrophic factor. Statistical analysis was performed by two-way ANOVA with Sidak's test for multiple comparisons (****$p < 0.0001$ vs control condition).

Table 4. IC_{50} Values of CIT, PEA, GDNF, Empty, and Loaded Microparticles (MPs) Were Calculated at 24, 48, and 72 h after MTT Experiments[a]

	IC_{50} (mg/mL)		
drug	24 h	48 h	72 h
MP EMPTY	$2.47 \times 10^{-4} \pm 5 \times 10^{-5}$	$2.49 \times 10^{-4} \pm 1.80 \times 10^{-5}$	$2.62 \times 10^{-4} \pm 3.4 \times 10^{-5}$
CIT	$1.02 \times 10^{-4} \pm 1 \times 10^{-5}$	$1.01 \times 10^{-4} \pm 1 \times 10^{-5}$	$1.09 \times 10^{-4} \pm 1.1 \times 10^{-5}$
MP CIT	$2.54 \times 10^{-4} \pm 2.1 \times 10^{-5}$	$2.60 \times 10^{-4} \pm 1.1 \times 10^{-5}$	$2.97 \times 10^{-4} \pm 2.5 \times 10^{-5}$
PEA	$9.7 \times 10^{-5} \pm 1.8 \times 10^{-5}$	$2.96 \times 10^{-4} \pm 3.6 \times 10^{-4}$	$1.06 \times 10^{-4} \pm 1.9 \times 10^{-5}$
MP PEA	$2.26 \times 10^{-4} \pm 4.4 \times 10^{-5}$	$2.83 \times 10^{-4} \pm 6.9 \times 10^{-5}$	$2.98 \times 10^{-4} \pm 9.3 \times 10^{-5}$
GDNF	$3.04 \times 10^{-4} \pm 9.9 \times 10^{-5}$	$3.49 \times 10^{-4} \pm 1.38 \times 10^{-4}$	$3.19 \times 10^{-4} \pm 5.9 \times 10^{-5}$
MP GDNF	$2.24 \times 10^{-4} \pm 3.6 \times 10^{-5}$	$2.39 \times 10^{-4} \pm 3.3 \times 10^{-5}$	$2.30 \times 10^{-4} \pm 5.8 \times 10^{-5}$

[a]IC_{50} values are expressed as mean ± SD ($n = 4$).

not significantly different between three drug-loaded MPs compared to unloaded ones.

4. DISCUSSION

Therapy of the diseases of the posterior eye segment necessitates an effective concentration of the chosen active molecules for long times in the target site. The concept of local administration by biodegradable MPs able to sustain the release of loaded drug(s) has been arising as an alternative to the repeated intravitreal injection of non-encapsulated active molecule(s).[34]

In this work, we have formulated HA-coated, PLGA-based degradable MPs for the sustained release of GDNF, PEA, and CIT by means of a fabrication technique already used to produce nanoparticles, with slight modifications. In these previous publications, the existence of the HA corona was assessed by means of ζ potential, ELISA kit, atomic force microscopy (AFM), and surface-enhanced Raman scattering (SERS) spectroscopy.[35,36] With regards to micrometric devices, the presence of HA on MP surface was assessed by Electron dispersive X-ray spectroscopy (EDS)[9] and, furthermore, by determining the diffusion properties of MPs in simulated vitreous body (SVB).[8] Results indicated that, with the same formulation proposed in this work, HA presence hindered the transport of MPs in SVB, probably due to the interactions of HA on MPs with the same polysaccharide in the gel. This can be attributed to the enhanced chemical affinity between MP corona and SVB. This is an important outcome since freely diffusing MPs may interfere with the visus and lead to blurred vision. These promising results have encouraged us to continue the studies to also verify their safety, both *in vitro* and *in vivo*. Thus, in this work, we have discussed the safety assessment of PLGA-based, HA-decorated MPs for intravitreal injection to verify the potential risks and benefits of the produced MPs. This investigation helps to shed light on the potential risk of inflammation, infection, and tissue damage inherent to MP administration.

This outcome holds significance because MPs that are allowed to move freely can disrupt vision and lead to blurred vision.

MPs produced by the double emulsion−solvent evaporation technique allow sustained drug release and provide protection of proteins from denaturation,[34] with a formulation selected in a previously published paper,[10] were loaded with CIT, PEA, or GDNF. BSA has been employed in the production of biodegradable MPs to safeguard GDNF from potential inactivation or denaturation upon encountering the polymeric matrix. Specifically, the quantity of BSA present in the

https://doi.org/10.1021/acs.biomac.3c00276
Biomacromolecules 2023, 24, 3510−3521

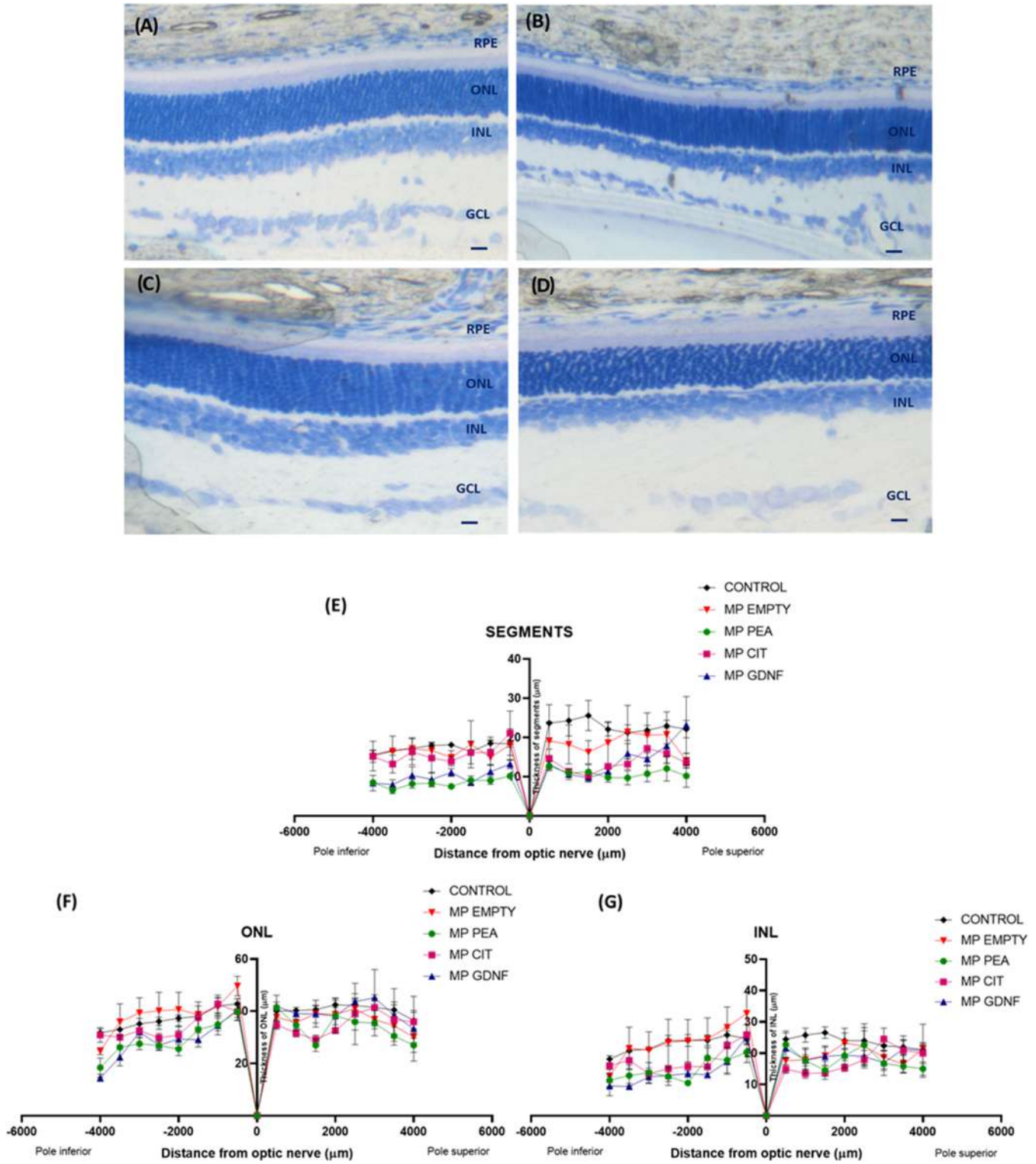

Figure 5. Retina thickness representative images from male rats injected with empty MPs (A) or MPs loaded with CIT (B), PEA (C), and GDNF (D). The scale bar is 10 μm. GCL, ganglion cell layer; INL, inner nuclear layer; ONL, outer nuclear layer; RPE, retinal pigmented epithelium. Effects of MP formulations on retinal thickness of segments (E), ONL (F), and INL (G). Values are presented as means ± SD (n = 4−5). Statistical analysis was performed by Kruskal−Wallis's test with Dunn's test for multiple comparisons. The injected doses to perform *in vivo* experiments were: 0.32 μg of PEA, 3.1 μg of CIT, and 46.1 ng of GDNF.

microparticles largely exceeds that of GDNF, increasing the probability of interaction with the organic matrix in comparison to GDNF. This protective mechanism ensures the preservation of the growth factor biological activity throughout the experimental timeframe.[27,37,38]

The entrapment efficiency ranged from 9 to 68%, and was heavily dependent on the nature of the encapsulated molecule, probably because of the different affinity between each active molecule and the inner organic phase of the emulsion used to produce the MPs. Different molecules were also associated

https://doi.org/10.1021/acs.biomac.3c00276
Biomacromolecules 2023, 24, 3510−3521

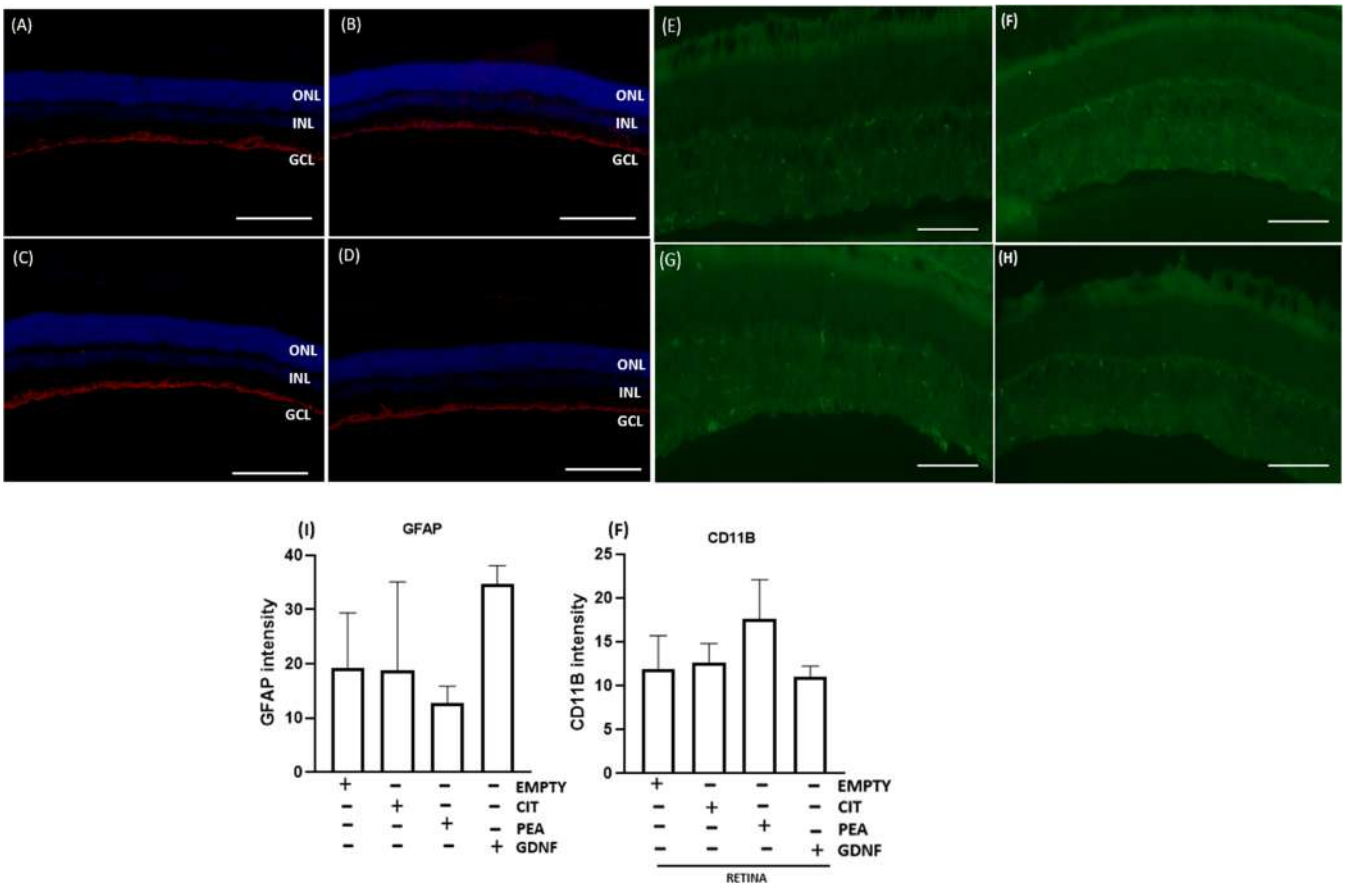

Figure 6. Representative images of MP EMPTY (A;E), MPs CIT (B;F), MPs PEA (C;G), and MPs GDNF (D;H). Scale bar: 50 μm. INL, inner nuclear layer; ONL, outer nuclear layer; GCL, ganglion cell layer. 4′,6-Diamidino-2-phenylindole (DAPI) stained blue the nuclei in ONL; GFAP stained red the astrocytes in GCL. CD11b stained resident retinal macrophages, the microglia, and infiltrated macrophages. The graphs (I) and (H) report the intensity level of GFAP and CD11b of MP EMPTY or loaded with CIT, PEA, and GDNF. Values are showed as means ± SD (n = 4).

with obvious morphological changes, as clearly shown in SEM micrographs. Specifically, the surface of CIT-loaded MPs exhibited noticeable pores. This can be explained by the high hydrophilicity of CIT and its significantly higher quantity compared to GDNF and PEA. Taking into account the values of encapsulation efficiency, CIT content is 3492-fold higher tha GDNF and 41.7-fold higher higher than PEA. Consequently, the polymeric matrix of CIT-loaded MPs is more hydrophilic compared to other formulations and therefore, during the evaporation step, the organic solvent is removed more rapidly. This, in turn, results in the formation of noticeable porosities on the external regions of the MPs.[28]

The loading efficiency of GDNF within the MPs (68%) was satisfactory, being higher than previous findings in the literature (approximately ranging from 29 to 49%), where the neurotrophic factor was loaded into MPs composed solely of PLGA.[27,38] This can be reasonably attributed to the presence of amphiphilic poloxamers within the polymeric matrix of MPs that can encourage interactions with hydrophilic active molecules. Another contributing factor to the high encapsulation efficiency is the high concentration of polymers in the organic matrix of the MPs. This results in an increased viscosity of the polymeric solution, which restricts GDNF migration toward the external aqueous phase of the emulsion used to produce MPs. In comparison to GDNF, CIT and PEA exhibit significantly lower loading efficiencies. The diminished loading efficiency of CIT, a highly hydrophilic molecule, can be attributed to its lower molecular weight (488 Da) when compared to GDNF (approximately 30 kDa) which, correspondingly, facilitates its migration outward. On the other hand, the low efficiency observed for PEA indicates an extensive loss of the active molecule during MP production.

MP mean size is suitable for injecting the suspension by means of a standard needle (31G). Additionally, a sustained GDNF release for at least two months was obtained. Differently, we found that the release of PEA and CIT is not effectively controlled, thus underlining that GDNF is the only molecule among the three studied that benefits from loading into biodegradable MPs. In detail, the release profile of GDNF from MPs exhibits a moderate initial burst, with a release rate range of 20−50 pg GDNF/mg MPs/day. This characteristic provides clear advantages compared to MPs composed solely of PLGA.[38] The favorable release behavior can be attributed to the thorough mixing between the active molecule and the polymer matrix, which limits the localization of the loaded protein near the surface of the MPs and reduces the burst effect. More in detail, the mechanism of drug release from MPs developed in this study involves a combination of drug diffusion and MP degradation. In the case of polymers that undergo bulk degradation, such as PLGA, water absorption leads to chain lysis throughout the matrix, thereby resulting in a decrease in average molecular weight.[39] However, the overall mass of MPs remains relatively stable until the polymer chains reach a small enough size to become soluble and diffuse out of

https://doi.org/10.1021/acs.biomac.3c00276
Biomacromolecules 2023, 24, 3510−3521

the matrix.[40] The rate of this process depends on the initial molecular weight of the polymer and the composition of the polymer matrix. In a recent study, we provided evidence that the incorporation of poloxamers into the PLGA matrix has dual effects on the degradation/erosion of MPs. First, poloxamers enhance the hydrophilicity of the MPs, thus promoting their erosion. However, at the same time, they dilute the PLGA, reducing the autocatalytic effects that contribute to erosion, thus delaying it. Consequently, this interplay between factors results in a steady and prolonged release profile.[10] The nearly zero order release observed for GDNF indicates that controlled degradation and increased MP hydrophilicity caused by poloxamers are fairly balanced in the produced MPs throughout the investigated release timeframe.

Also, as shown in the results paragraph, this controlled amount of GDNF showed a lack of cytotoxicity on ARPE-19 cell viability in 3 days, which could be correlated to its intrinsic neuroprotective activity. *In vitro* studies performed in this work were conducted with the aim of figuring out the possible cytotoxic and apoptotic effects of MPs on ARPE-19 cells. The comparison with the positive control (cisplatin) clearly indicated that the MPs are not toxic *in vitro* against ARPE-19 cells. Altogether, results proved that intravitreal injection of the produced MPs does not induce toxic effects on retinal neurons. This confirmed the safety of use and the biocompatibility of the devices obtained with a view to releasing drugs to the posterior segment of the eye.

In vivo safety experiments also showed no inflammatory response due to the lack of activation of Müller glial cells and microglia cells. Interestingly, the outcomes were similar for all groups, underlining that irrespective of the presence/absence of each active molecule, the MPs were safe *in vivo*.

5. CONCLUSIONS

The rational treatment of posterior eye segment diseases by intravitreal injections requires careful consideration of mitigating undesirable effects associated with this administration route. This necessitates precise control over the release kinetics of active molecules within the intravitreal space, ensuring sustained delivery. Achieving this control involves the meticulous design of micrometric devices capable of delivering these molecules at minute levels within the vitreous body. In this study, we have proved that the produced MPs can effectively sustain the release of GDNF at a fairly constant rate for several weeks, while showing a limited control over the release kinetics of PEA and CIT. The safety of MPs was verified through MTT and cytofluorimetric analysis, which showed the absence of cytotoxicity in ARPE-19 cells. Notably, the uncontrolled administration of GDNF resulted in decreased cell viability, while the sustained release of this molecule exhibited a positive effect in this regard, and this strongly underlines the need for GDNF encapsulation within biodegradable MPs.

These findings were further supported by *in vivo* measurements of rat retina thickness and immunohistochemical analysis, which revealed no significant impact on retina histology following intravitreal injection of both unloaded and loaded MPs.

This approach can be extended to other therapeutic molecules, including potential combinations, to facilitate a multi-drug therapy approach. In conclusion, the designed MPs have demonstrated great promise as a safe platform for delivering active molecules to the posterior segment of the eye.

A forthcoming study will expand on the findings of this research by exploring the therapeutic effects of GDNF encapsulated in the produced MPs. The investigation will involve examining a diverse range of drug concentrations, and the outcomes will be detailed in an upcoming publication.

■ ASSOCIATED CONTENT

Supporting Information

The Supporting Information is available free of charge at https://pubs.acs.org/doi/10.1021/acs.biomac.3c00276.

Chemical structures of CIT, PEA, PLGA, and HA (S1) and chromatograms and calibration curves of CIT (S2) and PEA (S3) are provided (DOC) (PDF)

■ AUTHOR INFORMATION

Corresponding Author

Marco Biondi − *Department of Pharmacy, University of Naples Federico II, 80131 Naples, Italy; Interdisciplinary Research Centre on Biomaterials (CRIB), 80125 Naples, Italy;* orcid.org/0000-0001-7299-9958; Email: mabiondi@unina.it

Authors

Teresa Silvestri − *Department of Pharmacy—Pharmaceutical Sciences, University of Bari Aldo Moro, 70125 Bari, Italy; Department of Pharmacy, University of Naples Federico II, 80131 Naples, Italy*

Alejandra Daruich − *Centre de Recherche des Cordeliers, INSERM UMRS1138, Team "From Physiopathology of Ocular Diseases to Clinical Development", Sorbonne Université, Université Paris Cité, 75006 Paris, France; Ophthalmology Department, Necker-Enfants Malades University Hospital, 75015 Paris, France*

Fatima Domenica Elisa De Palma − *Department of Molecular Medicine and Medical Biotechnologies, University of Napoli Federico II, 80131 Naples, Italy; Centre de Recherche des Cordeliers, INSERM UMRS1138, Université Paris Cité, Sorbonne Université, Team "Metabolism, Cancer & Immunity", 75006 Paris, France; Cell Biology and Metabolomics platforms, Gustave Roussy Cancer Campus, 94805 Villejuif, France*

Valentina Mollo − *Italian Institute of Technology—Centre for Advanced Biomaterials for Healthcare, 80125 Naples, Italy*

Marie Christine Naud − *Centre de Recherche des Cordeliers, INSERM UMRS1138, Team "From Physiopathology of Ocular Diseases to Clinical Development", Sorbonne Université, Université Paris Cité, 75006 Paris, France*

Danilo Aleo − *Medivis Srl, 95030 Tremestieri etneo, Catania, Italy*

Fabiola Spitaleri − *Medivis Srl, 95030 Tremestieri etneo, Catania, Italy*

Guido Kroemer − *Centre de Recherche des Cordeliers, INSERM UMRS1138, Université Paris Cité, Sorbonne Université, Team "Metabolism, Cancer & Immunity", 75006 Paris, France; Cell Biology and Metabolomics platforms, Gustave Roussy Cancer Campus, 94805 Villejuif, France*

Francine Behar-Cohen − *Centre de Recherche des Cordeliers, INSERM UMRS1138, Team "From Physiopathology of Ocular Diseases to Clinical Development", Sorbonne Université, Université Paris Cité, 75006 Paris, France*

Emilie Picard − *Centre de Recherche des Cordeliers, INSERM UMRS1138, Team "From Physiopathology of Ocular*

https://doi.org/10.1021/acs.biomac.3c00276
Biomacromolecules 2023, 24, 3510−3521

Diseases to Clinical Development", Sorbonne Université, Université Paris Cité, 75006 Paris, France

Maria Chiara Maiuri − *Department of Molecular Medicine and Medical Biotechnologies, University of Napoli Federico II, 80131 Naples, Italy; Centre de Recherche des Cordeliers, INSERM UMRS1138, Université Paris Cité, Sorbonne Université, Team "Metabolism, Cancer & Immunity", 75006 Paris, France; Cell Biology and Metabolomics platforms, Gustave Roussy Cancer Campus, 94805 Villejuif, France*

Laura Mayol − *Interdisciplinary Research Centre on Biomaterials (CRIB), 80125 Naples, Italy; Department of Advanced Biomedical Sciences, University of Naples Federico II, 80131 Naples, Italy*

Complete contact information is available at: https://pubs.acs.org/10.1021/acs.biomac.3c00276

Author Contributions

‡‡Co-last authors. T.S., M.B., and L.M. prepared and analyzed the MPs. T.S., D.A., and F.S. analyzed MPs by HPLC. V.M. analyzed MPs by SEM. T.S., F.D.E.D.P., and M.C.M. performed and analyzed the *in vitro* experiments. T.S., E.P., M.C.M., and A.D. carried out and analyzed the *in vivo* experiments and histological assays. T.S., E.P., and A.D. performed the statistical analysis. M.B., M.C.M., E.P., and L.M. conceived the study. T.S., E.P., F.D.E.D.P., M.C.M., M.B., and L.M. designed the study. L.M., M.B., M.C.M., E.P., G.K., and F.B.C. supervised the study. All authors contributed to writing the paper.

Funding

This work was supported by the grant entitled "Progettazione e sviluppo di microparticelle polimeriche per il rilascio prolungato di fattori di crescita nel corpo vitreo per il trattamento di malattie del segmento posteriore dell'occhio" within P.O.R. CAMPANIA FSE 2014/2020 (Campania Region, Italy), which funded the industrial PhD student (T.S.).

Notes

The authors declare no competing financial interest.

D.A. and F.S. are employees of Medivis Srl. PhD of TS was supported by an industrial grant and spent some time at Medivis Srl during her internship. All other authors declare no conflict of interest.

■ ACKNOWLEDGMENTS

The authors thank the CRC Core Facilities and Prof. Paolo Antonio Netti (Italian Institute of Technology) for providing the SEM apparatus.

■ LIST OF ABBREVIATIONS

ARPE:human retinal pigment epithelial cell line
ARVO:Association for Research in Vision and Ophthalmology
BSA:bovine serum albumin
CISPL:cisplatin
CIT:citicoline
CTRL:control
DAPI:4′,6-diamidino-2-phenylindole
EE:entrapment efficiency
GCL:ganglion cell layer
GDNF:glial-cell-derived neurotrophic factor
GRAS:generally regarded as safe
HA:hyaluronic acid
INL:inner nuclear layer
IVT:intravitreal injection
MPs:microparticles
MP EMPTY:microparticles empty
MP CIT:microparticles citicoline
MP PEA:microparticles palmitoylethanolamide
MP GDNF:microparticles GDNF
MTT:3-(4,5-dimethylthiazol-2-yl)-2,5-diphenyltetrazolium bromide
O.C.T.:optimal cutting temperature
O.D.:optical density
ONL:outer nuclear layer
PEA:palmitoylethanolamide
PLGA:polylactic-co-glycolic acid
PLGA MPs:polylactic-co-glycolic acid microparticles
RGCs:retinal ganglion cells
RPE:retinal pigmented epithelium
SEM:scanning electron microscopy
SVB:simulated vitreous body

■ REFERENCES

(1) Edelhauser, H. F.; Rowe-Rendleman, C. L.; Robinson, M. R.; Dawson, D. G.; Chader, G. J.; Grossniklaus, H. E.; Rittenhouse, K. D.; Wilson, C. G.; Weber, D. A.; Kuppermann, B. D.; Csaky, K. G.; Olsen, T. W.; Kompella, U. B.; Holers, V. M.; Hageman, G. S.; Gilger, B. C.; Campochiaro, P. A.; Whitcup, S. M.; Wong, W. T. Ophthalmic Drug Delivery Systems for the Treatment of Retinal Diseases: Basic Research to Clinical Applications. *Invest. Ophthalmol. Visual Sci.* **2010**, *51*, 5403−5420.

(2) Varela-Fernández, R.; Díaz-Tomé, V.; Luaces-Rodríguez, A.; Conde-Penedo, A.; García-Otero, X.; Luzardo-álvarez, A.; Fernández-Ferreiro, A.; Otero-Espinar, F. J. Drug Delivery to the Posterior Segment of the Eye: Biopharmaceutic and Pharmacokinetic Considerations. *Pharmaceutics* **2020**, *12*, No. 269.

(3) Klein, R.; Klein, B. E.; Linton, K. L. Prevalence of Age-Related Maculopathy: The Beaver Dam Eye Study. *Ophthalmology* **1992**, *99*, 933−943.

(4) Morello, C. M. Etiology and Natural History of Diabetic Retinopathy: An Overview. *Am. J. Health-Syst. Pharm.* **2007**, *64*, S3−S7.

(5) Bodor, N.; Buchwald, P. Ophthalmic Drug Design Based on the Metabolic Activity of the Eye: Soft Drugs and Chemical Delivery Systems. *AAPS J.* **2005**, *7*, E820−E833.

(6) Gaudana, R.; Ananthula, H. K.; Parenky, A.; Mitra, A. K. Ocular Drug Delivery. *AAPS J.* **2010**, *12*, 348−360.

(7) Ghasemi Falavarjani, K.; Nguyen, Q. D. Adverse Events and Complications Associated with Intravitreal Injection of Anti-VEGF Agents: A Review of Literature. *Eye* **2013**, *27*, 787−794.

(8) Mayol, L.; Silvestri, T.; Fusco, S.; Borzacchiello, A.; De Rosa, G.; Biondi, M. Drug Micro-Carriers with a Hyaluronic Acid Corona toward a Diffusion-Limited Aggregation within the Vitreous Body. *Carbohydr. Polym.* **2019**, *220*, 185−190.

(9) Serri, C.; Frigione, M.; Ruponen, M.; Urtti, A.; Borzacchiello, A.; Biondi, M.; Itkonen, J.; Mayol, L. Electron Dispersive X-Ray Spectroscopy and Degradation Properties of Hyaluronic Acid Decorated Microparticles. *Colloids Surf., B* **2019**, *181*, 896−901.

(10) Silvestri, T.; Immirzi, B.; Dal Poggetto, G.; Di Donato, P.; Mollo, V.; Mayol, L.; Biondi, M. How Poloxamer Addition in Hyaluronic-Acid-Decorated Biodegradable Microparticles Affects Polymer Degradation and Protein Release Kinetics. *Appl. Sci.* **2021**, *11*, 7567.

(11) Whitcup, S. M.; Robinson, M. R. Development of a Dexamethasone Intravitreal Implant for the Treatment of Non-infectious Posterior Segment Uveitis. *Ann. N. Y. Acad. Sci.* **2015**, *1358*, 1−12.

(12) Borzacchiello, A.; Mayol, L.; Schiavinato, A.; Ambrosio, L. Effect of Hyaluronic Acid Amide Derivative on Equine Synovial Fluid Viscoelasticity. *J. Biomed. Mater. Res., Part A* **2010**, *92*, 1162−1170.

(13) Chang, W.-H.; Liu, P.; Lin, M.; Lu, C.; Chou, H.; Nian, C.; Jiang, Y.; Hsu, Y. H. Applications of Hyaluronic Acid in Ophthalmology and Contact Lenses. *Molecules* **2021**, *26*, 2485.
(14) Puglia, C.; Blasi, P.; Ostacolo, C.; Sommella, E.; Bucolo, C.; Platania, C. B. M.; Romano, G. L.; Geraci, F.; Drago, F.; Santonocito, D.; Albertini, B.; Campiglia, P.; Puglisi, G.; Pignatello, R. Innovative Nanoparticles Enhance N-Palmitoylethanolamide Intraocular Delivery. *Front. Pharmacol.* **2018**, *9*, No. 285.
(15) Parisi, V.; Oddone, F.; Ziccardi, L.; Roberti, G.; Coppola, G.; Manni, G. Citicoline and Retinal Ganglion Cells: Effects on Morphology and Function. *Curr. Neuropharmacol.* **2018**, *16*, 919−932.
(16) Harada, C.; Harada, T.; Quah, H. M. A.; Maekawa, F.; Yoshida, K.; Ohno, S.; Wada, K.; Parada, L. F.; Tanaka, K. Potential Role of Glial Cell Line-Derived Neurotrophic Factor Receptors in Müller Glial Cells during Light-Induced Retinal Degeneration. *Neuroscience* **2003**, *122*, 229−235.
(17) Paterniti, I.; Di Paola, R.; Campolo, M.; Siracusa, R.; Cordaro, M.; Bruschetta, G.; Tremolada, G.; Maestroni, A.; Bandello, F.; Esposito, E.; Zerbini, G.; Cuzzocrea, S. Palmitoylethanolamide Treatment Reduces Retinal Inflammation in Streptozotocin-Induced Diabetic Rats. *Eur. J. Pharmacol.* **2015**, *769*, 313−323.
(18) Gagliano, C.; Ortisi, E.; Pulvirenti, L.; Reibaldi, M.; Scollo, D.; Amato, R.; Avitabile, T.; Longo, A. Ocular Hypotensive Effect of Oral Palmitoyl-Ethanolamide: A Clinical Trial. *Investig. Ophthalmol. Visual Sci.* **2011**, *52*, 6096−6100.
(19) Grieb, P. Neuroprotective Properties of Citicoline: Facts, Doubts and Unresolved Issues. *CNS Drugs* **2014**, *28*, 185−193.
(20) Wells, A. J.; Viaroli, E.; Hutchinson, P. J. The Management of Traumatic Brain Injury. *Surgery* **2021**, *39*, 470−478.
(21) Fresina, M.; Dickmann, A.; Salerni, A.; De Gregorio, F.; Campos, E. C. Effect of Oral CDP-Choline on Visual Function in Young Amblyopic Patients. *Graefe's Arch. Clin. Exp. Ophthalmol.* **2008**, *246*, 143−150.
(22) Bogdanov, P.; Sampedro, J.; Solà-Adell, C.; Simó-Servat, O.; Russo, C.; Varela-Sende, L.; Simó, R.; Hernández, C. Effects of Liposomal Formulation of Citicoline in Experimental Diabetes-Induced Retinal Neurodegeneration. *Int. J. Mol. Sci.* **2018**, *19*, 2458.
(23) Matteucci, A.; Varano, M.; Gaddini, L.; Mallozzi, C.; Villa, M.; Pricci, F.; Malchiodi-Albedi, F. Neuroprotective Effects of Citicoline in in Vitro Models of Retinal Neurodegeneration. *Int. J. Mol. Sci.* **2014**, *15*, 6286−6297.
(24) Park, C. H.; Yoon, S. K.; Hae, S. N.; Eun, W. C.; Young, A. Y.; Ji, M. Y.; Wan, S. C.; Cho, G. J. Neuroprotective Effect of Citicoline against KA-Induced Neurotoxicity in the Rat Retina. *Exp. Eye Res.* **2005**, *81*, 350−358.
(25) Fudalej, E.; Justyniarska, M.; Kasarełło, K.; Dziedziak, J.; Szaflik, J. P.; Cudnoch-Jędrzejewska, A. Neuroprotective Factors of the Retina and Their Role in Promoting Survival of Retinal Ganglion Cells: A Review. *Ophthalmic Res.* **2021**, *64*, 345−355.
(26) Hauck, S. M.; Kinkl, N.; Deeg, C. A.; Swiatek-de Lange, M.; Schöffmann, S.; Ueffing, M. GDNF Family Ligands Trigger Indirect Neuroprotective Signaling in Retinal Glial Cells. *Mol. Cell. Biol.* **2006**, *26*, 2746−2757.
(27) Arranz-Romera, A.; Esteban-Pérez, S.; Molina-Martínez, I. T.; Bravo-Osuna, I.; Herrero-Vanrell, R. Co-Delivery of Glial Cell−Derived Neurotrophic Factor (GDNF) and Tauroursodeoxycholic Acid (TUDCA) from PLGA Microspheres: Potential Combination Therapy for Retinal Diseases. *Drug Delivery Transl. Res.* **2021**, *11*, 566−580.
(28) García-Caballero, C.; Lieppman, B.; Arranz-Romera, A.; Molina-Martínez, I. T.; Bravo-Osuna, I.; Young, M.; Baranov, P.; Herrero-Vanrell, R. Photoreceptor Preservation Induced by Intravitreal Controlled Delivery of Gdnf and Gdnf/Melatonin in Rhodopsin Knockout Mice. *Mol. Vision* **2018**, *24*, 733−745.
(29) Beck-Broichsitter, M.; Paulus, I. E.; Greiner, A.; Kissel, T. Modified Vibrating-Mesh Nozzles for Advanced Spray-Drying Applications. *Eur. J. Pharm. Biopharm.* **2015**, *92*, 96−101.
(30) Dureau, P.; Bonnel, S.; Menasche, M.; Dufier, J. L.; Abitbol, M. Quantitative Analysis of Intravitreal Injections in the Rat. *Curr. Eye Res.* **2001**, *22*, 74−77.
(31) Aldossary, S. A. Review on Pharmacology of Cisplatin: Clinical Use, Toxicity and Mechanism of Resistance of Cisplatin. *Biomed. Pharmacol. J.* **2019**, *12*, 7−15.
(32) Sarthy, P. V.; Fu, M.; Huang, J. Developmental Expression of the Glial Fibrillary Acidic Protein (GFAP) Gene in the Mouse Retina. *Cell. Mol. Neurobiol.* **1991**, *11*, 623−637.
(33) Huang, W.; Hu, F.; Wang, M.; Gao, F.; Xu, P.; Xing, C.; Sun, X.; Zhang, S.; Wu, J. Comparative Analysis of Retinal Ganglion Cell Damage in Three Glaucomatous Rat Models. *Exp. Eye Res.* **2018**, *172*, 112−122.
(34) Herrero-Vanrell, R.; Bravo-Osuna, I.; Andrés-Guerrero, V.; Vicario-de-la-Torre, M.; Molina-Martínez, I. T. The Potential of Using Biodegradable Microspheres in Retinal Diseases and Other Intraocular Pathologies. *Prog. Retinal Eye Res.* **2014**, *42*, 27−43.
(35) Giarra, S.; Serri, C.; Russo, L.; Zeppetelli, S.; De Rosa, G.; Borzacchiello, A.; Biondi, M.; Ambrosio, L.; Mayol, L. Spontaneous Arrangement of a Tumor Targeting Hyaluronic Acid Shell on Irinotecan Loaded PLGA Nanoparticles. *Carbohydr. Polym.* **2016**, *140*, 400−407.
(36) La Verde, G.; Sasso, A.; Rusciano, G.; Capaccio, A.; Fusco, S.; Mayol, L.; Biondi, M.; Silvestri, T.; Netti, P. A.; La Commara, M.; Panzetta, V.; Pugliese, M. Characterization of Hyaluronic Acid-Coated PLGA Nanoparticles by Surface-Enhanced Raman Spectroscopy. *Int. J. Mol. Sci.* **2023**, *24*, No. 601.
(37) Garbayo, E.; Ansorena, E.; Lanciego, J. L.; Aymerich, M. S.; Blanco-prieto, M. J. Sustained Release of Bioactive Glycosylated Glial Cell-Line Derived Neurotrophic Factor from Biodegradable Polymeric Microspheres. *Eur. J. Pharm. Biopharm.* **2008**, *69*, 844−851.
(38) Arranz-Romera, A.; Hernandez, M.; Checa-Casalengua, P.; Garcia-Layana, A.; Molina-Martinez, I. T.; Recalde, S.; Young, M. J.; Tucker, B. A.; Herrero-Vanrell, R.; Fernandez-Robredo, P.; Bravo-Osuna, I. A Safe Gdnf and Gdnf/Bdnf Controlled Delivery System Improves Migration in Human Retinal Pigment Epithelial Cells and Survival in Retinal Ganglion Cells: Potential Usefulness in Degenerative Retinal Pathologies. *Pharmaceuticals* **2021**, *14*, No. 50.
(39) Biondi, M.; Indolfi, L.; Ungaro, F.; Quaglia, F.; La Rotonda, M. I.; Netti, P. A. Bioactivated Collagen-Based Scaffolds Embedding Protein-Releasing Biodegradable Microspheres: Tuning of Protein Release Kinetics. *J. Mater. Sci.: Mater. Med.* **2009**, *20*, 2117−2128.
(40) Netti, P. A.; Biondi, M.; Frigione, M. Experimental Studies and Modeling of the Degradation Process of Poly(Lactic-Co-Glycolic Acid) Microspheres for Sustained Protein Release. *Polymers* **2020**, *12*, 2042.

https://doi.org/10.1021/acs.biomac.3c00276
Biomacromolecules 2023, 24, 3510−3521